

See discussions, stats, and author profiles for this publication at: <https://www.researchgate.net/publication/51557545>

# Vibrational and Valence Photoelectron Spectroscopies, Matrix Photochemistry, and Conformational Studies of ClC(O)SSCl

ARTICLE in THE JOURNAL OF PHYSICAL CHEMISTRY A · AUGUST 2011

Impact Factor: 2.69 · DOI: 10.1021/jp204789h · Source: PubMed

---

READS

20

## 6 AUTHORS, INCLUDING:



**Yeny Tobon Correa**

Université des Sciences et Technologies de L...

32 PUBLICATIONS 116 CITATIONS

SEE PROFILE



**Weigang Wang**

Chinese Academy of Sciences

69 PUBLICATIONS 471 CITATIONS

SEE PROFILE



**Mao-Fa Ge**

Chinese Academy of Sciences

259 PUBLICATIONS 3,020 CITATIONS

SEE PROFILE



**Carlos O. Della Vedova**

National University of La Plata

293 PUBLICATIONS 2,678 CITATIONS

SEE PROFILE

# Vibrational and Valence Photoelectron Spectroscopies, Matrix Photochemistry, and Conformational Studies of ClC(O)SSCl

Yeny A. Tobón,<sup>†</sup> Melina V. Cozzarín,<sup>†</sup> Wei-Gang Wang,<sup>‡</sup> Mao-Fa Ge,<sup>‡</sup> Carlos O. Della Védova,<sup>†,§</sup> and Rosana M. Romano<sup>\*,†</sup>

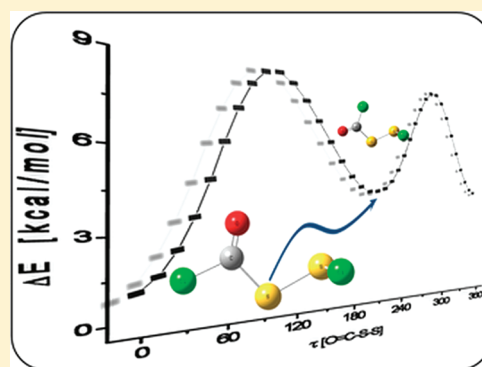
<sup>†</sup>CEQUINOR (UNLP-CONICET, CCT-La Plata), Departamento de Química, Facultad de Ciencias Exactas, Universidad Nacional de La Plata, C.C. 962, 1900 La Plata, Argentina

<sup>‡</sup>Beijing National Laboratory for Molecular Sciences (BNLMS), State Key Laboratory for Structural Chemistry of Unstable and Stable Species, Institute of Chemistry, Chinese Academy of Sciences, 100190, Beijing, P. R. China

<sup>§</sup>LaSeISiC (CIC-UNLP-CONICET), Departamento de Química, Facultad de Ciencias Exactas, Universidad Nacional de La Plata, Camino Centenario y 508, 1897 Gonnet, Argentina

 Supporting Information

**ABSTRACT:** ClC(O)SSCl was prepared by an improved method by the reaction of  $[(\text{CH}_3)_2\text{CHOC}(\text{S})]_2\text{S}$  with  $\text{SO}_2\text{Cl}_2$  in hexane. The photoelectron spectra in the gas phase present four distinct regions, corresponding to ionizations from electrons formally located at the S, O, and Cl atoms and at the C=O bond. The vibrational IR and Raman spectra of the liquid were interpreted in terms of the most stable syn-gauche conformer (the O=C double bond syn with respect to the S—S single bond and the C—S single bond gauche with respect to the S—Cl single bond) in equilibrium with the less stable anti-gauche form, both occurring in two enantiomeric forms. The randomization process between the conformers was induced by broad-band UV–visible irradiation in matrix conditions, and several photoproducts were identified by FTIR spectroscopy. The experimental results were complemented by theoretical calculations.



## INTRODUCTION

It is well established that molecules possessing the XC(O)S— group, with X = halogen, present two potential energy minima corresponding to the syn and anti forms, the syn conformer always being the most stable one (see, for example, ref 1 and references cited therein). When X is a chlorine atom, the energy differences between the anti and syn conformers prevent the detection of the anti form by experimental methods as IR and Raman spectroscopy and gas electron diffraction studies. However, the second conformer was experimentally observed in some compounds through the matrix isolation technique in a very low proportion at ambient temperature (<1%), and confirmed by the randomization process induced by UV–visible light.<sup>2–4</sup> On the other hand, it is also well-known that molecules with a disulfide bond adopt a gauche conformation around the S—S bond.

(Chlorocarbonyl)disulfanyl chloride, ClC(O)SSCl, was prepared by the first time by Böhme in 1981.<sup>17</sup> Although it has been identified by three of its fundamental absorptions in the IR spectrum, as far as we know no vibrational, electronic, or conformational studies on this compound were reported.

In this paper we present an improved method for the preparation of ClC(O)SSCl. The conformational properties were predicted by DFT methods and used as a starting point for the interpretation of the experimental results. The photoelectron spectra of the vapor phase were recorded and interpreted in terms of the most

stable conformer. The assignment of the bands was performed by the comparison with the theoretical predictions and also by comparison with related molecules. A complete vibrational study, including the IR and Raman spectra of the liquid sample and the FTIR spectra of the compound isolated in solid matrixes (Ar and N<sub>2</sub>) was consistent with the presence of the most stable conformer in equilibrium with the second one, responsible for some very weak features in the spectra. The matrixes were irradiated to confirm the assignment of the absorptions to the second conformer, through the randomization process. Exposed to UV–visible light, ClC(O)SSCl isolated in solid matrixes decomposes following different unimolecular mechanisms. The different photoproducts were identified by means of their FTIR spectra in matrix conditions, and the photochemical mechanisms proposed.

## EXPERIMENTAL SECTION

**Sample Preparation.** Reagents and solvents were purchased reagent grade and used without further purification, with the exception of  $\text{SO}_2\text{Cl}_2$  that was purified by distillation.  $[(\text{CH}_3)_2\text{CHOC}(\text{S})]_2\text{S}$  was prepared according to literature procedures.<sup>5</sup>

**Received:** May 23, 2011

**Revised:** August 3, 2011

**Published:** August 10, 2011

In this work, the methods reported in the literature<sup>6–8</sup> for the synthesis of  $\text{ClC}(\text{O})\text{SSCl}$  were improved by reducing the number of steps and the reaction time. A mixture of  $[(\text{CH}_3)_2\text{CHOC}(\text{S})]_2\text{S}$  (10 mmol),  $\text{SO}_2\text{Cl}_2$  (30 mmol), and  $\text{CaCO}_3$  (100 mg) in hexane (10 mL) was refluxed at 75 °C for 3.5 h, then filtered, and concentrated on a rotary evaporator. The reaction was followed by GC–MS.  $(\text{CH}_3)_2\text{CHOC}(\text{S})\text{SSC}(\text{O})\text{Cl}$  was identified as an intermediate product that disappears after 3 h of reaction. The resulting oil was found to consist of around 78% of  $\text{ClC}(\text{O})\text{SSCl}$  and 22% of  $\text{ClC}(\text{O})\text{SSSC}(\text{O})\text{Cl}$ . The sample was purified by repeated trap-to-trap distillations in vacuum giving pure  $\text{ClC}(\text{O})\text{SSCl}$ .

**Gas Chromatography–Mass Spectrometry.** A GC–MS Shimadzu QP-2010 was used to record the mass spectra in

$\text{CCl}_4$  solutions. Further details are given in the Supporting Information.

**Photoelectron Spectroscopy.** The photoelectron spectrum was recorded on a double-chamber UPS-II machine, which was designed specifically to detect transient species as described elsewhere,<sup>9,10</sup> at a resolution of about 30 meV indicated by the standard  $\text{Ar}^+({}^2\text{P}_{3/2})$  photoelectron band. Experimental vertical ionization energies were calibrated with methyl iodide.

**FTIR Spectroscopy.** The liquid FTIR spectra of  $\text{ClC}(\text{O})\text{SSCl}$  were recorded on a Nexus Nicolet instrument equipped with either an MCTB or a DTGS detector (for the ranges 4000–400 or 600–100  $\text{cm}^{-1}$ , respectively) at ambient temperature using KBr, CsI, or polyethylene windows.

**FT-Raman Spectroscopy.** A Bruker IFS66 was used to record the FT-Raman spectra of the liquid sample in a capillary tube at ambient temperature between 3500 and 100  $\text{cm}^{-1}$ , with a resolution of 4  $\text{cm}^{-1}$  and 1024 scans.

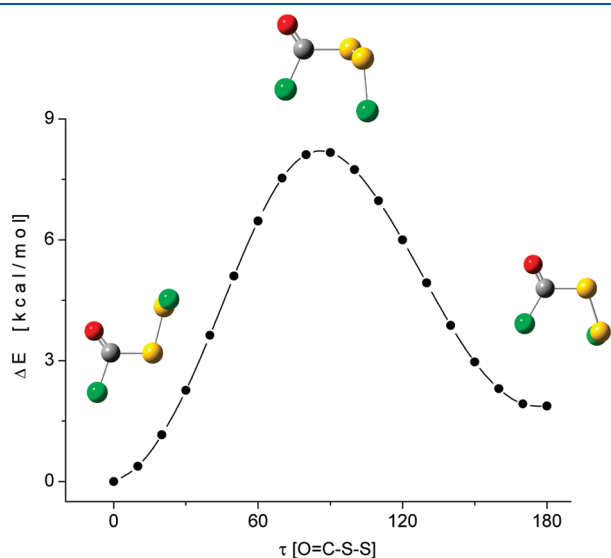


**Figure 1.** Potential energy curve for  $\text{ClC}(\text{O})\text{SSCl}$  around the C–S single bond from 0 to 180° in steps of 10° calculated at the B3LYP/6-31+G\* level of approximation by a relaxed scan, with a starting value for the CSSCl dihedral angle of 90°.

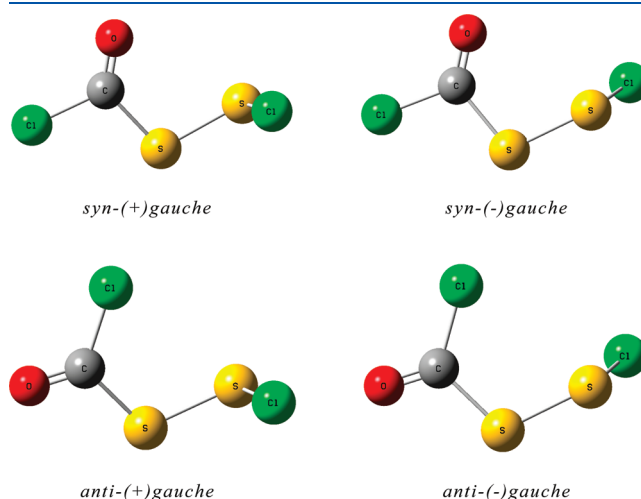


**Figure 3.** syn–gauche and anti–gauche conformers of  $\text{ClC}(\text{O})\text{SSCl}$  in two enantiomeric forms each, calculated with the B3LYP/6-31+G\* approximation.

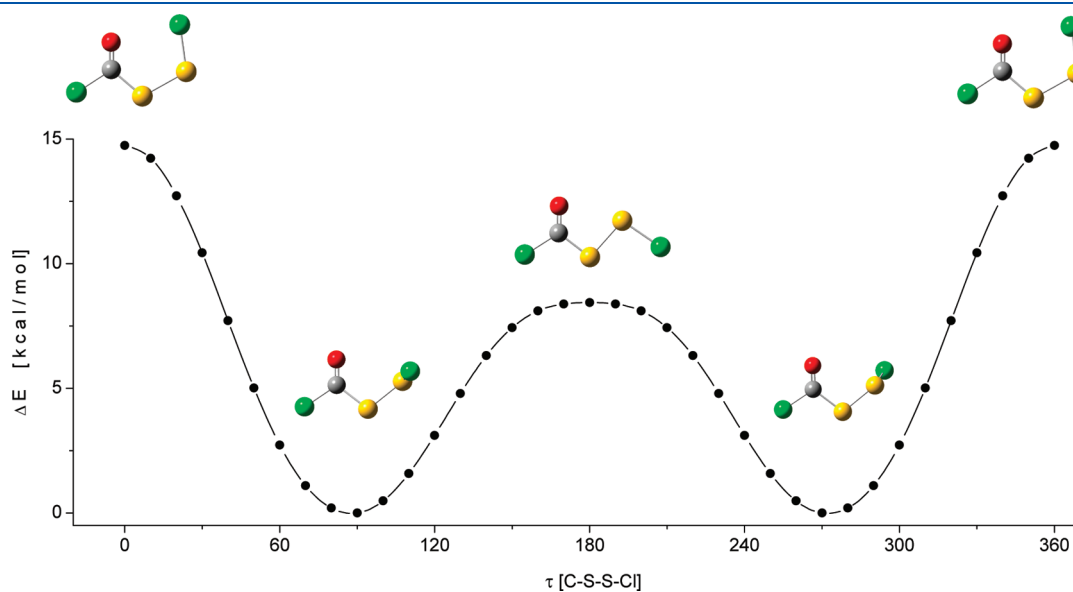


**Figure 2.** Potential energy curve for syn- $\text{ClC}(\text{O})\text{SSCl}$  around the S–S single bond from 0 to 360° in steps of 10° calculated at the B3LYP/6-31+G\* level of approximation by a relaxed scan.

**Table 1.** Energy and Free Energy Differences between the Two Conformers of ClC(O)SSCl (kcal mol<sup>-1</sup>) and Relative Proportions of the Rotamers at Ambient Temperature Calculated with Different Theoretical Approximations

theoretical model	$\Delta E^0$ (anti-gauche-syn-gauche)	$\Delta G^0$ (anti-gauche-syn-gauche)	% syn-gauche	% anti-gauche
B3LYP/6-31+G*	1.87	1.84	95.7	4.3
MP2/6-31+G*	2.22	2.20	97.6	2.4

**Table 2.** Experimental Vertical Ionization Energies (IP, eV) of ClC(O)SSCl, Computed Vertical Ionization Energies ( $E_v$ , eV) at the OVGF/6-31+G\* Level of Approximation and Molecular Orbital Characters for the syn-gauche Conformer of ClC(O)SSCl

IP (eV)	$E_v$ (eV)	MO	characters
10.10 <sup>a</sup>	9.96	40	$n_{\pi}S$ (S-C)
10.25 <sup>a</sup>	10.80	39	$n_{\pi}S$ (S-Cl)
11.42	11.61	38	$n_{\sigma}O$
12.15 <sup>a</sup>	11.96	37	$n_{\pi}Cl$ (Cl-S)
12.34 <sup>a</sup>	12.36	36	$n_{\pi}Cl$ (Cl-C)
12.57 <sup>a</sup>	12.39	35	$n_{\sigma}Cl$ (Cl-C)
12.81 <sup>a</sup>	13.10	34	$n_{\sigma}Cl$ (Cl-S-S)
14.17	13.88	33	$\pi_{C=O}$

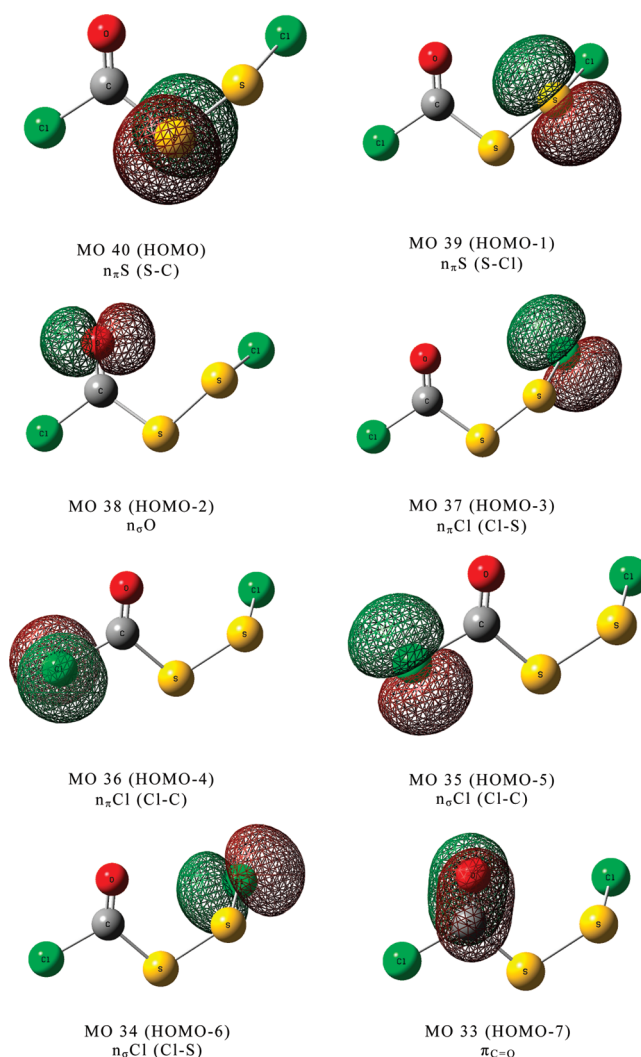
<sup>a</sup> Value obtained from the deconvolution of the PES spectrum (Figure 5).

**Matrix Isolation and Photochemical Studies.** Gas mixtures of ClC(O)SSCl with Ar or N<sub>2</sub> (both AGA) in the proportion ca. 1:1000, prepared by standard manometric methods, were deposited on a CsI window cooled to ca. 15 K by means of a Displex closed-cycle refrigerator (SHI-APD Cryogenics, model DE-202) using the pulse deposition technique.<sup>11,12</sup> The matrix isolated FTIR spectra were recorded on a Nexus Nicolet instrument equipped with either an MCTB or a DTGS detector (for the ranges 4000–400 or 600–180 cm<sup>-1</sup>, respectively). Following deposition and IR analysis of the resulting matrix, the sample was exposed to broad-band UV–visible radiation (200 <  $\lambda$  < 800 nm) from a Spectra-Physics Hg–Xe arc lamp operating at 1000 W. The output from the lamp was limited by a water filter to absorb IR radiation and so minimize any heating effects. The IR spectra of the matrix with 0.5 and 0.125 cm<sup>-1</sup> resolution were then recorded at different times of irradiation to monitor closely any change in the spectra.

**Theoretical Calculations.** All of the quantum chemical calculations were performed using the Gaussian 03 program system.<sup>13</sup> Geometry optimizations were sought using standard gradient techniques by simultaneous relaxation of all the geometrical parameters. The calculated vibrational properties correspond in all cases to potential energy minima for which no imaginary vibrational frequency was found. The vertical ionization energies ( $E_v$ ) were calculated according to Cederbaum's outer valence Green's function (OVGF) method with the 6-31+G\* basis set, on the basis of the B3LYP/6-31+G\* optimized geometry.

## RESULTS AND DISCUSSION

**Theoretical Calculations.** The conformational properties of ClC(O)SSCl were investigated through different potential energy scans using the B3LYP/6-31+G\* theoretical approximation. In the first place, the potential energies were calculated by the simultaneous relaxation of all geometric parameters with the exception of the O=C–S–S torsional angle, which was varied from 0 to 180°, in steps of 10°. The starting value for the C–S–

**Figure 4.** Schematic representation and approximate assignment of the eighth highest occupied molecular orbitals of the syn-gauche conformer of ClC(O)SSCl.

S–Cl dihedral angle was set to 90°. As observed in Figure 1, two stable conformers, the syn and anti forms (the orientation of the O=C double bond with respect to the S–S single bond), were found as minima in the potential energy curve, with an energy barrier of 8.16 kcal mol<sup>-1</sup>. Subsequently, the potential energy curve generated by the rotation of the S–S single bond was calculated for the syn (Figure 2) and anti (Figure S1 of the Supporting Information) conformers. As expected by the presence of the disulfide bond, two minima were obtained in each of the potential energy curves, corresponding to two enantiomeric forms. The energy barrier between the two minima, as calculated with the B3LYP/6-31+G\* approximation, was 8.44 and 9.17 kcal mol<sup>-1</sup> for the syn and anti forms, respectively.



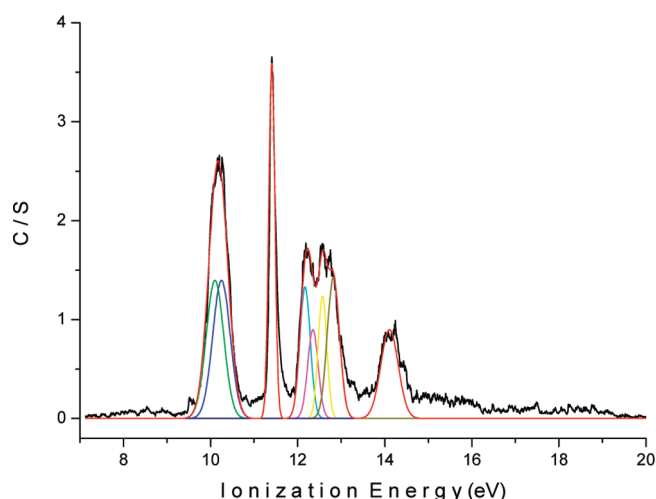


Figure 5. He I photoelectron spectrum of ClC(O)SSCl and individual peaks after deconvolution of the spectrum.

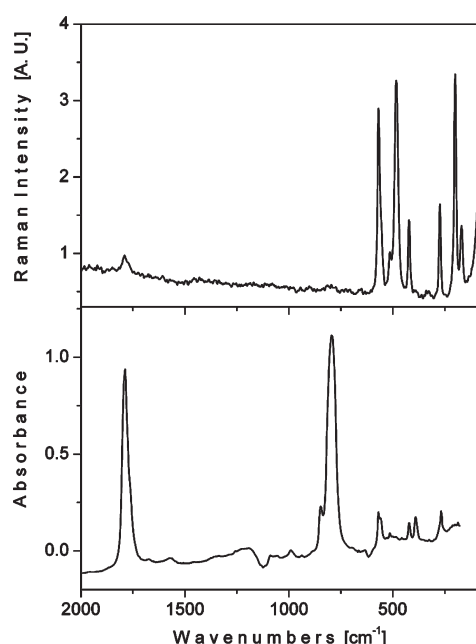


Figure 6. Liquid FTIR (bottom) and FTRaman (top) spectra of ClC(O)SSCl.

The structures corresponding to minima over the potential energy scans were fully optimized using the B3LYP and MP2 approximation, in combination with the 6-31+G\* basis set. Figure 3 shows the syn-gauche (the O=C double bond syn with respect to the S—S single bond and the C—S single bond gauche with respect to the S—Cl single bond) and the anti-gauche conformers, occurring in two enantiomeric forms. The ClC(O)SS— moiety presents a planar structure in both conformers. The calculated theoretical parameters are placed as Supporting Information (Table S1).

The syn-gauche form is predicted invariably to be the more stable one by about 2 or 3 kcal mol<sup>−1</sup> depending on the theoretical model used for the calculation, which corresponds of a vapor phase containing less than 5% of the higher energy anti-gauche form at room temperature. Table 1 resumes the energy and free

energy differences between the two conformers as well as the relative proportions of the rotamers at ambient temperature as predicted by different theoretical models.

The vibrational properties of the syn-gauche and anti-gauche conformers were calculated by the B3LYP and MP2 theoretical methods in combination with the 6-31+G\* basis set (for a complete list of the wavenumbers, IR and Raman relative intensities, and tentative assignment see Tables S2 and S3 of the Supporting Information). The vibrational normal modes predicted as the most sensitive to the conformation are the  $\nu(\text{C}=\text{O})$  and  $\nu_{\text{as}}(\text{Cl}-\text{C}-\text{S})$  fundamentals. Accordingly, with the B3LYP/6-31+G\* calculations, the  $\nu(\text{C}=\text{O})$  vibrations are expected to occur around 1864 (syn-gauche) and 1832 (anti-gauche) cm<sup>−1</sup>, and the  $\nu_{\text{as}}(\text{Cl}-\text{C}-\text{S})$  normal modes are predicted at 796 (syn-gauche) and 840 (anti-gauche) cm<sup>−1</sup>.

OVGF calculations in combination with the 6-31+G\* basis set were performed for the most stable syn-gauche conformer using the structural parameters optimized at the B3LYP/6-31+G\* level. The first eight vertical ionization energies are listed in Table 2, and Figure 4 shows a schematic representation and approximate assignment of the eight highest occupied molecular orbitals of the syn-gauche conformer of ClC(O)SSCl.

**Photoelectron Spectroscopy.** The He I photoelectron spectrum of ClC(O)SSCl between 7 and 20 eV is presented in Figure 5. The experimental spectrum was deconvoluted into eight individual peaks, also shown in Figure 5. The experimentally observed ionization energies (IP in eV), measured at the maxima of each of the deconvoluted peaks, are summarized in Table 2. The analysis and assignment of the spectrum was based on the calculated vertical ionization energies at the OVGF/6-31+G\* level of approximation for the most stable syn-gauche conformer because, according to different theoretical calculations presented above, the vapor is predicted to be composed of this form by at least 95%.

As observed in Figure 5, the photoelectron spectrum of ClC(O)SSCl can be clearly divided into four regions. The first band in the spectrum, occurring as a broad feature near 10.2 eV, can be interpreted as the overlap of two peaks at about 10.10 and 10.25 eV, arising from ionizations of molecular orbitals localized on the sulfur atoms. This assignment is in agreement with previous reports of photoelectron spectra of other disulfides, for which the first ionizations were also assigned to the outermost 3p lone pair of the sulfur atoms. For example, the first two vertical ionization energies of CF<sub>3</sub>C(O)OSSOC(O)CF<sub>3</sub> were reported to occur at 10.81 and 10.97 eV and assigned to the outermost p orbitals of the sulfur atoms,<sup>14</sup> and for CH<sub>3</sub>C(O)OSSOC(O)CH<sub>3</sub> the bands were observed at 9.83 and 9.95 eV.<sup>15</sup>

The second band in the photoelectron spectrum appearing at 11.40 eV presents a narrow and sharp contour, characteristic of ionization from an essentially nonbonding orbital. According to the prediction of the calculations, this band is assigned to ionization from the nonbonding orbital of the oxygen atom. This assignment is in agreement with the one proposed for the 11.32 eV band in the photoelectron spectrum of ClC(O)SCI.<sup>16</sup>

The third group of bands, located between 12 and 13 eV, are assigned to ionizations originated in the chlorine atoms. According to the theoretical predictions, four different bands are expected in this region, arising from ionizations located in the  $n\sigma$  and  $n\pi$  orbital of each of the chlorine atoms of the molecule. After deconvolution of the spectrum, bands at around 12.17, 12.35, 12.57, and 12.82 eV were assigned to  $n_{\pi}\text{Cl}$  (Cl—S—S),  $n_{\pi}\text{Cl}$  (Cl—C=O),  $n_{\sigma}\text{Cl}$  (Cl—C=O), and  $n_{\sigma}\text{Cl}$  (Cl—S—S), respectively, following

**Table 3.** Experimental (Liquid IR and Raman and Ar and N<sub>2</sub> Matrixes) and Calculated (B3LYP/6-31+G\*) Wavenumbers (cm<sup>−1</sup>) for ClC(O)SSCl

Experimental				B3LYP/ 6-31+G*			Assignment
FTIR	FT-Raman	Ar-matrix	N <sub>2</sub> - matrix	Wavenumbers	I IR	I Raman	
1788	1790	1805.6 1804.5 1803.4 1798.5 1795.9 1775.5	1808.1 1806.2 1804.4 1801.7 1799.0 1796.9 1787.4 1775.5	1864	58	61	$\nu$ (C=O) <i>syn-gauche</i>
1763	1772	1722.7 1721.6	1740.2 1736.6	1832	98	100	$\nu$ (C=O) <i>anti-gauche</i>
1570							2 $\nu_{as}$ (Cl-C-S) <i>syn-gauche</i>
1673							2 $\nu_{as}$ (Cl-C-S) <i>anti-gauche</i>
847		851.3 850.1 847.6	856.5	840	100	2	$\nu_{as}$ (Cl-C-S) <i>anti-gauche</i>
794	797	812.3 803.2 801.8 800.8 796.6 794.4	815.0 810.8 807.3 805.6 803.6	796	100	8	$\nu_{as}$ (Cl-C-S) <i>syn-gauche</i>
568	569	589.3	588.0	567	1	12	$\delta_{oop}$ (C=O) <i>syn-gauche</i>
557	557	571.2 560.5	566.5	554	3	61	$\nu_s$ (Cl-C-S) <i>syn-gauche</i>
483	483	492.2	497.2 491.4	495	<1	11	$\nu$ (S-S) <i>syn-gauche</i>
422	422	455.4 449.2	461.0 464.4 456.5 448.2	450	13	100	$\nu$ (S-Cl) <i>syn-gauche</i>
390	391			414	4	18	$\delta$ (Cl-C=O) <i>syn-gauche</i>
268	274			270	2	13	$\delta$ (Cl-C-S) <i>syn-gauche</i>
	201			190	<1	29	$\delta$ (S-S-Cl) <i>syn-gauche</i>
	169			162	<1	5	$\delta$ (C-S-S) <i>syn-gauche</i>

the trend predicted by the calculations. These values are also in agreement with the reported vertical ionizations from the electrons formally located at the chlorine atoms in ClC(O)SCl.<sup>16</sup> However, it is interesting to compare the order of the ionization energies in the latter molecule,  $n_{\pi}\text{Cl}(\text{Cl}-\text{C}=\text{O}) < n_o\text{Cl}(\text{Cl}-\text{C}=\text{O}) < n_{\pi}\text{Cl}(\text{Cl}-\text{S}) < n_o\text{Cl}(\text{Cl}-\text{S})$ , with respect to the proposed one for ClC(O)SSCl,  $n_{\pi}\text{Cl}(\text{Cl}-\text{S}-\text{S}) < n_{\pi}\text{Cl}(\text{Cl}-\text{C}=\text{O}) < n_o\text{Cl}(\text{Cl}-\text{C}=\text{O}) < n_o\text{Cl}(\text{Cl}-\text{S}-\text{S})$ . As can be inferred from these trends, the ionization of electrons formally located at the  $\pi$  orbital of the Cl atom bonded to the S atom in ClC(O)SSCl results easier than in ClC(O)SCl, which may be associated with the loss of planarity in the former molecule.

The last feature in the spectrum, above 14 eV, was assigned to ionization from a  $\pi_{\text{C}=\text{O}}$  orbital, in accordance with both theoretical predictions and previously reported values for related molecules (see, for example, ref 16 and references cited therein).

**Vibrational Studies.** As mentioned in the Introduction, only three fundamentals of the IR spectrum of the title compound were reported in the literature, at 1795, 795, and 490 cm<sup>−1</sup>, and assigned to  $\nu(\text{C}=\text{O})$ ,  $\nu_{as}(\text{ClCS})$ , and  $\nu(\text{SS})$ , respectively.<sup>17</sup>

Here, we present a complete vibrational study of ClC(O)SSCl, including the IR and Raman spectra of the net liquid and the IR spectrum of the compound isolated in solid Ar and N<sub>2</sub> matrixes. The bands observed in the experimental spectra have been assigned on the basis of comparisons (i) with the calculated IR and Raman spectrum and (ii) with the spectra of related molecules, particularly ClC(O)SCl,<sup>3,4</sup> ClC(O)SSC(O)Cl,<sup>18</sup> ClC(O)SSSC(O)Cl,<sup>19</sup> ClC(O)SSCH<sub>3</sub>,<sup>20</sup> and ClC(O)SSCF<sub>3</sub>.<sup>20</sup>

The IR and Raman spectra of liquid ClC(O)SSCl are shown in Figure 6. In Table 3 the experimental wavenumbers, obtained from the liquid IR and Raman spectra and by Ar and N<sub>2</sub> matrixes, are compared with the calculated wavenumbers for the *syn-gauche* and *anti-gauche* conformers of ClC(O)SSCl using the B3LYP/6-31+G\* approximation. The complete simulated spectra using different approximations are given in Tables S2 and S3 in the Supporting Information.

The experimental IR and Raman spectra of ClC(O)SSCl were interpreted in terms of an equilibrium between the *syn-gauche* and *anti-gauche* conformers. Ten of the twelve fundamentals of the most stable *syn-gauche* were experimentally observed, the

other two being predicted below  $100\text{ cm}^{-1}$ , out of our experimental range, and assigned to the vibrational torsions around the S—S and C—S single bonds. On the other hand, the presence of

**Table 4. Wavenumbers and Assignments of the IR Absorptions Appearing after Broad-Band UV–Visible Photolysis of ClC(O)SSCl Isolated in an Ar Matrix**

Ar matrix $\nu\text{ [cm}^{-1}\text{]}$	Assignment Molecule	Vibrational mode	Wavenumbers reported previously
2140.8	OC...Cl <sub>2</sub>	$\nu\text{ (C=O)}$	2140.7 <sup>a</sup>
2138.4	CO	$\nu\text{ (C=O)}$	2138.2 <sup>a</sup>
2051.0	OCS...Cl <sub>2</sub> linear	$\nu\text{ (C=O)}$	2050.6 <sup>b</sup>
2049.6	free OCS	$\nu\text{ (C=O)}$	2049.6 <sup>b</sup>
2047.1	SCO...Cl <sub>2</sub>	$\nu\text{ (C=O)}$	2046.9 <sup>b</sup>
2042.0	OCS...Cl <sub>2</sub> angular	$\nu\text{ (C=O)}$	2042.0 <sup>b</sup>
1998.3	O <sup>13</sup> C...Cl <sub>2</sub>	$\nu\text{ (C=O)}$	1998.0 <sup>b</sup>
1996.9	O <sup>13</sup> CS	$\nu\text{ (C=O)}$	1997.0 <sup>b</sup>
1994.3	S <sup>13</sup> CO...Cl <sub>2</sub>	$\nu\text{ (C=O)}$	1994.3 <sup>b</sup>
1877.1	ClCO·	$\nu\text{ (C=O)}$	1876.7 <sup>c</sup>
1815.1 1814.1 1812.9 1810.1	OCCL <sub>2</sub>	$\nu\text{ (C=O)}$	1810.12 <sup>d</sup>
858.9	OSC	$\nu\text{ (C=S)}$	858.7 <sup>b</sup>
857.6	OCS...Cl <sub>2</sub> linear	$\nu\text{ (C=S)}$	857.1 <sup>b</sup>
837.4 836.6	OCCL <sub>2</sub>	$\nu_{\text{as}}\text{ (Cl-C-Cl)}\text{ (}\nu_{\text{s}}\text{)}$	837.36 837.20 <sup>d</sup>
520.4	SCl <sub>2</sub>	$\nu_{\text{s}}\text{ (}^{35}\text{ClS}^{35}\text{Cl)}$	520.2 <sup>c</sup>
517.3	SCl <sub>2</sub>	$\nu_{\text{as}}\text{ (}^{35}\text{ClS}^{35}\text{Cl)}$	517.5 <sup>c</sup>
515.5	SCl <sub>2</sub>	$\nu_{\text{s}}\text{ (}^{35}\text{ClS}^{37}\text{Cl)}$	515.2 <sup>c</sup>

<sup>a</sup> Reference 21. <sup>b</sup> Reference 23. <sup>c</sup> Reference 4. <sup>d</sup> Reference 25.

the second conformational form was discernible by the presence of two low intensity bands. This assignment was confirmed by their photochemical behavior in matrix conditions, as described below.

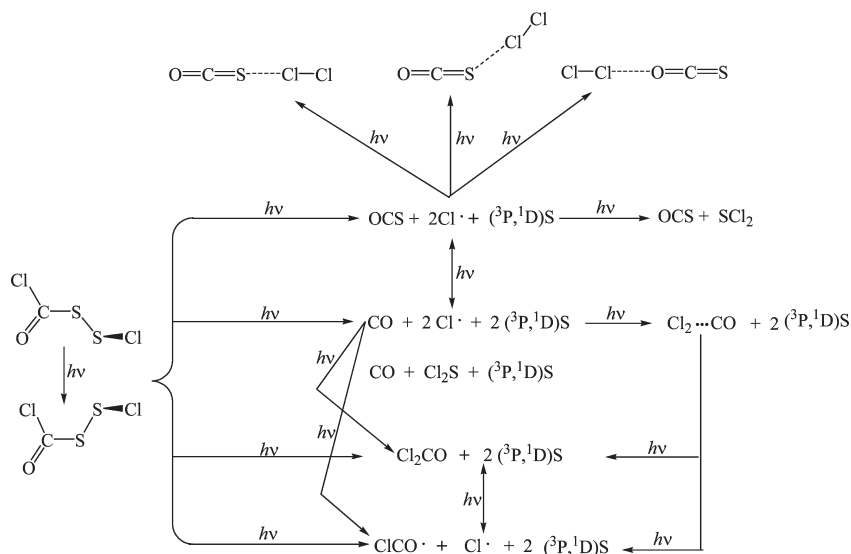
The most intense IR absorptions occur at  $794$  and  $1788\text{ cm}^{-1}$  in the liquid phase and at  $801.8$  and  $1804.5\text{ cm}^{-1}$  in the Ar matrix, in agreement with the predicted values of  $796.1$  and  $1863.6\text{ cm}^{-1}$  for the Cl—C—S antisymmetric stretching and C=O stretching, respectively, of the most stable syn—gauche conformer of ClC(O)SSCl. Additionally, both spectra in liquid phase and in matrix conditions show the features corresponding to the anti—gauche conformer in these regions at  $847\text{ cm}^{-1}$  (liquid) and  $847.6\text{ cm}^{-1}$  (Ar matrix) for the  $\nu_{\text{as}}\text{ (Cl—C—S)}$  mode and at  $1763\text{ cm}^{-1}$  (liquid) and  $1721.6\text{ cm}^{-1}$  (Ar matrix) for the  $\nu\text{ (C=O)}$  mode, which were observed to increase their intensities with the irradiation (see Matrix Isolation Photochemistry section below).

The most intense Raman bands of liquid ClC(O)SSCl were observed to occur around  $569$ ,  $483$ ,  $422$ ,  $274$ ,  $201$ , and  $169\text{ cm}^{-1}$ . Comparison with the results of the B3LYP/6-31+G\* calculations suggests that these features correspond to  $\delta_{\text{oop}}\text{ (C=O)}$ ,  $\nu\text{ (S—S)}$ ,  $\nu\text{ (S—Cl)}$ ,  $\delta\text{ (Cl—C—S)}$ ,  $\delta\text{ (S—S—Cl)}$ , and  $\delta\text{ (C—S—S)}$  modes of the syn—gauche form, respectively.

**Matrix Isolation Photochemistry.** Ar or N<sub>2</sub> matrixes doped with ClC(O)SSCl in an approximate proportion 1:1000 were irradiated with broad-band UV–visible light. The IR spectra for the matrix-isolated compound suggest the presence of more than one conformer, the syn—gauche form with the O=C—S—S dihedral angle close to  $0^\circ$  and the C—S—S—Cl dihedral angle near  $90^\circ$  being accompanied by a small proportion of the anti—gauche form with the O=C—S—S dihedral angle near to  $180^\circ$  and the C—S—S—Cl dihedral angle near  $90^\circ$ . Moreover, exposure of the matrix to broad-band UV–visible light resulted in growth of the absorptions associated with the second conformer at the expense of those associated with the syn—gauche form, in a process known as randomization (see ref 1 and references cited therein). This behavior reinforces the proposed assignment of the IR and Raman bands to the second conformer of ClC(O)SSCl in the spectra of the liquid sample.

Besides the observed randomization process, ClC(O)SSCl isolated in solid matrixes displays a very rich photochemistry.

**Scheme 1. Possible Mechanisms of the Photolysis Occurring in Ar or N<sub>2</sub> Matrixes Containing ClC(O)SSCl at  $\sim 15\text{ K}$**



Several new IR bands were observed to grow upon UV–visible irradiation of the matrixes, as presented in Table 4. The most distinctive of these new absorptions are those occurring in the region around 2138 and 2050  $\text{cm}^{-1}$ , identified as the photoelimination of  $\text{CO}^{21}$  and  $\text{OCS}^{22}$  respectively. The features appearing at 2140.8, 2051.0, 2047.1, and 2042.0  $\text{cm}^{-1}$  on photolysis, were recognized as complexes of CO or OCS previously reported, such as  $\text{OC}\cdots\text{Cl}_2$ ,<sup>21</sup>  $\text{OCS}\cdots\text{Cl}_2$  linear,  $\text{SCO}\cdots\text{Cl}_2$ , and  $\text{OCS}\cdots\text{Cl}_2$  angular,<sup>23</sup> respectively.

The formation of the  $\text{ClCO}^\bullet$  radical was identified by its characteristic sharp IR absorption near 1877  $\text{cm}^{-1}$ .<sup>24,4</sup> Phosgene,  $\text{OCCl}_2$ ,<sup>25,26</sup> and sulfur dichloride,  $\text{SCl}_2$ ,<sup>27,4</sup> were also detected by comparison of some of their most intense IR absorptions with reported values for these species isolated in solid matrixes or formed by photochemical matrix reactions.

Scheme 1 summarizes the photochemical channels of  $\text{ClC(O)SSCl}$  isolated in solid Ar and  $\text{N}_2$  matrixes, proposed on the basis of the identified photoproducts and the behavior of the IR absorption as a function of irradiation time. These channels include the syn–gauche  $\rightarrow$  anti–gauche randomization, the formation of the  $\text{ClCO}^\bullet$  radical, and decomposition to CO, OCS,  $\text{SCl}_2$ ,  $\text{OCCl}_2$ , and  $\text{Cl}_2$ , favoring the formation of molecular complexes.

**Mass Spectra.** The mass spectra of  $\text{ClC(O)SSCl}$  shows the  $\text{M}^+$  peak at  $m/q = 162$ , besides the typical peaks ( $\text{M} + 2$ ) and ( $\text{M} + 4$ ) of compounds containing two chlorine atoms. The fragments containing chlorine are also observed with the corresponding characteristic natural isotopic abundance. The most prominent fragments observed in the spectrum, such as  $\text{OCS}^+$  ( $m/q = 60$ ),  $\text{ClCO}^+$  ( $m/q = 63$ ),  $\text{SS}^+$  ( $m/q = 64$ ), and  $\text{ClSS}^+$  ( $m/q = 99$ ) are in agreement with the molecular structure (Figure S2 of the Supporting Information).

## CONCLUSIONS

In this paper we present an improved method for the preparation of  $\text{ClC(O)SSCl}$ , by decreasing the number of reaction steps and the proportion of the byproduct. A complete characterization using different experimental techniques, including vibrational spectroscopy (IR, Raman, and matrix-isolation IR), photoelectron spectroscopy, and mass spectrometry, was complemented by the results of theoretical calculations. The photo-decomposition channels under UV–visible irradiation were studied by IR matrix isolation photochemistry.

The vapor of  $\text{Cl(O)SSCl}$  at ambient temperature has been shown by vibrational spectroscopy to consist of an equilibrium mixture of syn–gauche and anti–gauche conformers, in accordance with theoretical calculations that predict a proportion around 95 and 5%, of these two forms, respectively. The photochemical induced randomization process observed in matrix conditions is again revealed as a very useful technique for experimental study of conformational equilibrium.

The photoelectron spectra of  $\text{ClC(O)SSCl}$  was analyzed in terms of the most stable syn–gauche conformer only. Aimed by theoretical predictions and the comparison with the electronic properties of related species, the PES spectrum was clearly divided into four distinct regions, attributable to ionizations arising from the nonbonding orbitals of the two S, O, and Cl atoms, and from the  $\pi_{\text{C=O}}$  orbital.

After broad band UV–visible irradiation of solid matrixes doped with  $\text{ClC(O)SSCl}$ , different reactions channels were identified. The course and sequence of these photolytic changes

have been traced through the IR spectrum of the matrixes, and the products were identified and characterized by their reported wavenumbers. The main photoproducts, detected as free or complexed species, were CO, OCS,  $\text{Cl}_2$ ,  $\text{Cl}_2\text{CO}$ , and  $\text{SCl}_2$ , together with the  $\text{ClCO}^\bullet$  radical. As reported previously, the confined conditions in the matrix cage especially favor the formation of molecular complexes.

## ASSOCIATED CONTENT

**S Supporting Information.** Cartesian coordinates of the optimized structures of the syn–gauche and anti–gauche conformers of  $\text{ClC(O)SSCl}$  and simulated vibrational spectra at the B3LYP/6-31+G\* and MP2/6-31+G\* level of approximations (Tables S1–S6), potential energy curve for anti- $\text{ClC(O)SSCl}$  around the S–S single bond from 0 to 360° in steps of 10° calculated at the B3LYP/6-31+G\* level of approximation by a relaxed scan (Figure S1) and experimental details of the Gas chromatography–mass spectrometry measurements and mass spectrum of  $\text{ClC(O)SSCl}$  (Figure S2). This material is available free of charge via the Internet at <http://pubs.acs.org>.

## AUTHOR INFORMATION

### Corresponding Author

\*E-mail: [romano@quimica.unlp.edu.ar](mailto:romano@quimica.unlp.edu.ar).

## ACKNOWLEDGMENT

C.O.D.V. and R.M.R. thank the Consejo Nacional de Investigaciones Científicas y Técnicas (CONICET) (PIP 0352), the Agencia Nacional de Promoción Científica y Tecnológica (ANPCyT) (PICT 33878 and 322), the Comisión de Investigaciones Científicas de la Provincia de Buenos Aires (CIC), and the Facultad de Ciencias Exactas, Universidad Nacional de La Plata, for financial support. R.M.R. is also grateful to the Fundación Antorchas. In addition, Y.A.T. acknowledges with thanks a Deutscher Akademischer Austauschdienst (DAAD) award.

## REFERENCES

- (1) Romano, R. M.; Della Védova, C. O.; Downs, A. J. *Chem.—Eur. J.* **2007**, *13*, 8185–8192.
- (2) Romano, R. M.; Della Védova, C. O.; Downs, A. J.; Greene, T. M. *J. Am. Chem. Soc.* **2001**, *123*, 5794–5801.
- (3) Romano, R. M.; Della Védova, C. O.; Downs, A. J.; Parsons, S.; Smith, C. *New J. Chem.* **2003**, *27*, 514–519.
- (4) Romano, R. M.; Della Védova, C. O.; Downs, A. J. *J. Phys. Chem. A* **2004**, *108*, 7179–7187.
- (5) Whitby, G. S.; F. R. S. C.; Gallay, W. *Trans. R. Soc. Can.* **1929**, *23*, 20–24.
- (6) Barany, G.; Mott, A. W. *J. Org. Chem.* **1984**, *49*, 1043–1051.
- (7) Chen, L.; Zouliková, I.; Slaninová, J.; Barany, G. *J. Med. Chem.* **1997**, *40*, 864–876.
- (8) Schroll, A. L.; Barany, G. *J. Org. Chem.* **1986**, *51*, 1866–1881.
- (9) Yao, L.; Ge, M.; Wang, W.; Zeng, X.; Sun, Z.; Wang, D. *Inorg. Chem.* **2006**, *45*, 5971–5975.
- (10) Du, L.; Yao, L.; Zeng, X.; Ge, M.; Wang, D. *J. Phys. Chem. A* **2007**, *111*, 4944–4949.
- (11) Almond, M. J.; Downs, A. J. *Adv. Spectrosc.* **1989**, *17*, 1–511. Dunkin, I. R. *Matrix-Isolation Techniques: A Practical Approach*; Oxford University Press: New York, 1998.
- (12) Perutz, R. N.; Turner, J. J. *J. Chem. Soc., Faraday Trans. 2* **1973**, *69*, 452–461.



(13) Frisch, M. J.; Trucks, G. W.; Schlegel, H. B.; Scuseria, G. E.; Robb, M. A.; Cheeseman, J. R.; Montgomery, J. A., Jr.; Vreven, T.; Kudin, K. N.; Burant, J. C.; Millam, J. M.; Iyengar, S. S.; Tomasi, J.; Barone, V.; Mennucci, B.; Cossi, M.; Scalmani, G.; Rega, N.; Petersson, G. A.; Nakatsuji, H.; Hada, M.; Ehara, M.; Toyota, K.; Fukuda, R.; Hasegawa, J.; Ishida, M.; Nakajima, T.; Honda, Y.; Kitao, O.; Nakai, H.; Klene, M.; Li, X.; Knox, J. E.; Hratchian, H. P.; Cross, J. B.; Adamo, C.; Jaramillo, J.; Gomperts, R.; Stratmann, R. E.; Yazyev, O.; Austin, A. J.; Cammi, R.; Pomelli, C.; Ochterski, J. W.; Ayala, P. Y.; Morokuma, K.; Voth, G. A.; Salvador, P.; Dannenberg, J. J.; Zakrzewski, V. G.; Dapprich, S.; Daniels, A. D.; Strain, M. C.; Farkas, O.; Malick, D. K.; Rabuck, A. D.; Raghavachari, K.; Foresman, J. B.; Ortiz, J. V.; Cui, Q.; Baboul, A. G.; Clifford, S.; Cioslowski, J.; Stefanov, B. B.; Liu, G.; Liashenko, A.; Piskorz, P.; Komaromi, I.; Martin, R. L.; Fox, D. J.; Keith, T.; Al-Laham, M. A.; Peng, C. Y.; Nanayakkara, A.; Challacombe, M.; Gill, P. M. W.; Johnson, B.; Chen, W.; Wong, M. W.; Gonzalez, C.; Pople, J. A. *Gaussian 03*, Revision B.04; Gaussian, Inc.: Pittsburgh, PA, 2003.

(14) Zeng, X.; Ge, M.; Sun, Z.; Wang, D. *J. Phys. Chem. A* **2006**, *110*, 5685–5691.

(15) Du, L.; Yao, L.; Ge, M. *J. Phys. Chem. A* **2007**, *111*, 11787–11792.

(16) Geronés, M.; Erben, M. F.; Romano, R. M.; Della Védova, C. O.; Yao, L.; Ge, M. *J. Phys. Chem. A* **2008**, *112*, 2228–2234.

(17) Böhme, H.; Brinkmann, M.; Steudel, H. *Liebigs Ann. Chem.* **1981**, 1244–1251.

(18) Ulic, S. E.; Aymonino, P. J.; Della Védova, C. O. *J. Raman Spectrosc.* **1991**, *22*, 675–678.

(19) Tobon, Y. A.; Cozzarín, M. V.; Romano, R. M.; Della Védova, C. O. *J. Mol. Struct.* **2009**, *930*, 37–42.

(20) Hermann, A.; Ulic, S. E.; Della Védova, C. O.; Mack, H.; Oberhammer, H. *J. Fluorine Chem.* **2001**, *112*, 297–305.

(21) Romano, R. M.; Downs, A. J. *J. Phys. Chem. A* **2003**, *107*, 5298–5305.

(22) Verderame, F. D.; Nixon, E. R. *J. Chem. Phys.* **1966**, *44*, 43–48. Hawkins, M.; Almond, M. J.; Downs, A. J. *J. Phys. Chem.* **1985**, *89*, 3326–3334. Lang, V. I.; Winn, J. S. *J. Chem. Phys.* **1991**, *94*, 5270–5274.

(23) Picone, A. L.; Romano, R. M.; Della Védova, C. O.; Willner, H.; Downs, A. J. *J. Phys. Chem. Chem. Phys.* **2010**, *12*, 563–571.

(24) Schnockel, H.; Eberlein, R. A.; Plitt, H. S. *J. Chem. Phys.* **1992**, *97*, 4–7.

(25) Mincu, I.; Allouche, A.; Cossu, M.; Aycard, J.-P.; Pourcin *J. Spectrochim. Acta, Part A* **1995**, *51*, 349–362.

(26) Romano, R. M.; Della Védova, C. O.; Downs, A. J.; Tobón, Y. A.; Willner, H. *Inorg. Chem. A* **2005**, *44*, 3241–3248.

(27) Bielefeldt, D.; Willner, H. *Spectrochim. Acta, Part A* **1980**, *36*, 989–995.